JOURNAL OF MATERIALS SCIENCE 16 (1981) 1088–1096

A probabilistic theory for the strength of short fibre composites

HIROSHI FUKUDA*, TSU-WEI CHOU
Mechanical and Aerospace Engineering Department, University of Delaware, Newark, Delaware 19711, USA

This paper presents a probabilistic theory for predicting the strength of unidirectional short fibre composites. It is assumed that the failure of the composite occurs due to the inability of the short fibres bridging a critical zone to carry the load. The stress concentrations on the fibres bridging a fibre end gap are evaluated as a function of the number of fibre ends forming the gap. The sizes of the gaps are predicted from a probabilistic approach. The short fibre composite strength is then estimated from the gap size and the corresponding stress concentration factor. Comparisons of the present work with existing theories and experiments have been made.

1. Introduction

Composite materials reinforced with discontinuous fibres have versatile properties and are relatively inexpensive to fabricate. The fibres are relatively short, variable in length and imperfectly aligned. Fibres including glass, graphite, Kevlar and asbestos have been used to reinforce polymeric matrices. As discussed by Chou and Kelly [1, 2], the strength and failure behaviour of short fibre composites are complicated by the non-uniformity in fibre length and orientation as well as by the interaction between the fibres and matrix at the fibre ends.

Several theories have been proposed to predict the strength of short fibre composites. One theory is based upon a modification of the "rule of mixtures" originally developed for continuous fibre composites. For unidirectional continuous fibre composites, under the assumption of iso-strain in the fibres and matrix, the rule of mixtures assumes the following form [3]

$$\sigma_{cu} = \sigma_{fu}V_f + \sigma'_m(1 - V_f), \qquad (1)$$

where σ_{cu} and σ_{fu} are the ultimate tensile strength of the composite and fibre, respectively, σ'_m is the matrix stress at the ultimate tensile strain of the fibres and V_f denotes fibre volume fraction.

In the case of short fibre composites, Equation 1 is modified as follows [3]

$$\sigma_{cu} = \sigma_{fu}V_f F(l_c/l) + \sigma'_m(1 - V_f), \qquad (2)$$

where l_c and l denote critical and actual fibre length, respectively. The factor, $F(l_c/l)$ which takes into account the effect of fibre length, is less than unity and

$$F(l_c/l) = 1 - (l_c/2l) \qquad (3)$$

for the case of constant interfacial shear stress.

It is an established fact that even in continuous fibre composites, failure can initiate when a micro-crack forms at the weakest point of a fibre. The works of Zweben [4], Fukuda and Kawata [5, 6] and Oh [7] have demonstrated this fact. The problem of discontinuous fibre composites is, however, complicated by the presence of fibre ends and the resulting stress concentration. Riley [8], taking into consideration the stress concentration due to fibre discontinuity, obtained the following expression for composite strength

$$\sigma_c = \frac{6/7}{1 + (5l_c/7l)}\sigma_f V_f + \sigma'_m(1 - V_f). \qquad (4)$$

Although his approach is an oversimplified one, the basic idea of load transfer seems to be important.

A systematic experimental study of short fibre composite strength was performed by Curtis,

*On leave from the Institute of Space and Aeronautical Science, University of Tokyo, Japan.

 0022–2461/81/041088–09$02.90/0

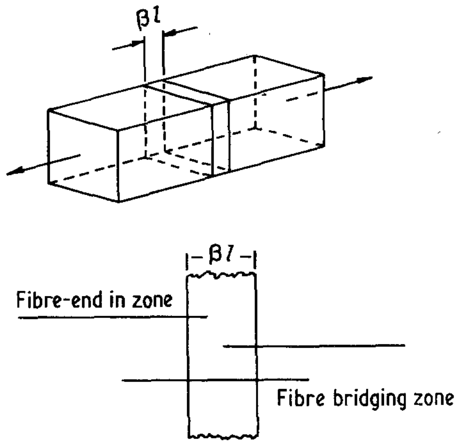

Figure 1 A typical critical zone in a short fibre composite (after [10]).

Bader and Bailey [9] using polyamide thermoplastic reinforced with short glass and graphite fibres. These findings of Curtis, Bader and Bailey [9] led Bader, Chou and Quigley [10] to propose a damage model. The basic concepts are that microcracks are most likely to develop at fibre ends at microscopic strains well below the fibre failure strain, and that failure is finally initiated in a critical cross-section that has been weakened by the accumulation of cracks.

Fig. 1 depicts a typical volume element in a short fibre composite used by Bader, Chou and Quigley [10]. The width of a "critical zone" in the strength model is denoted by βl where β is a constant parameter and l is the average fibre length. The number of fibre ends within the critical zone, and the number of fibres bridging the zone are functions of the critical zone width. The strength of the composite is determined by the relative numbers of fibres that bridge the zone versus those with ends within the zone. These latter will develop matrix cracks when the strain exceeds a critical value. The critical situation arises when the bridging fibres are unable to sustain the load transfer due to matrix cracking and failure occurs. The critical stress and strain values for a wide range of fibre aspect ratio, fibre critical length, fibre–matrix interfacial strength and critical zone width have been evaluated by Bader, Chou and Quigley [10].

In this paper, a probabilistic approach is adopted to examine the strength of unidirectional short fibre composites. The probability of finding a number of fibre ends clustered together forming a "fibre end gap" is derived as a function of gap size. The stress concentrations on fibres bridging a fibre end gap are taken into account in deriving the strength of the composite. It should be noted that this strength theory based upon the probabilistic approach gives the *average* strength obtainable from a large number of test specimens.

2. Theory

2.1. Modifications of the rule of mixtures

A unidirectional short fibre composite material where the fibres are of uniform length and strength is considered. The mechanisms of failure can be categorized according to fibre length (Fig. 2). When fibres are very short, a crack formed at a fibre end can circumvent the neighbouring fibres without breaking them (Fig. 2a). Final failure of the composite is then attributed to fibre pull-out. On the other hand, if fibres are sufficiently long, fibre end cracks will cause fracture of the neighbouring fibres and hence, failure of the composite (Fig. 2b). A strength model based upon the latter case is described in this paper.

The composite ultimate strength σ_{cu} is defined as the stress level which causes first fibre fracture. Consequently, the maximum stress in a fibre is of primary importance in predicting composite strength. Fig. 3 schematically shows stress distributions in a short fibre. Here, σ_{max} and σ_0 are the maximum and plateau stresses of the profile.

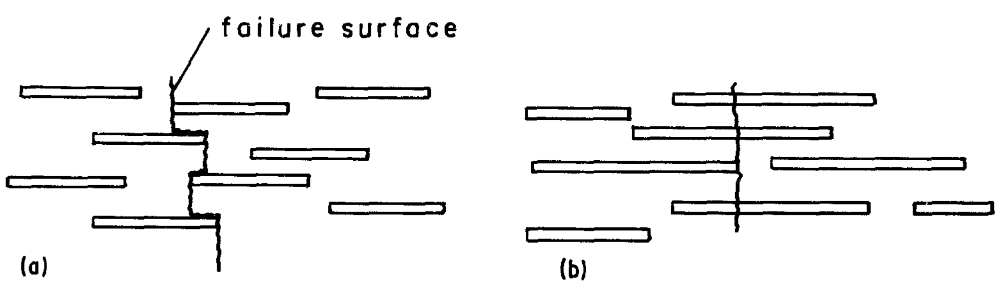

Figure 2 Two failure modes in short fibre composites.

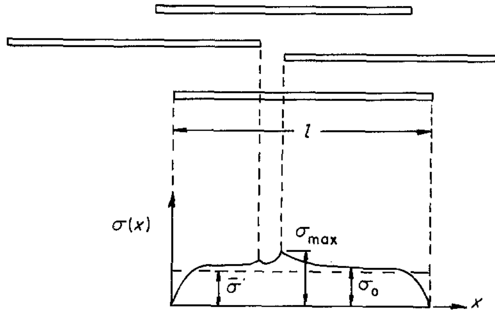

Figure 3 Stress distribution in a short fibre.

The average fibre stress at failure is given by

$$\bar{\sigma} = \frac{1}{l}\int_0^l \sigma(x)\,dx. \tag{5}$$

In the case where the composite has a distribution of fibre lengths, Equation 5 should be replaced by

$$\bar{\sigma} = \int_0^\infty f(l)\left(\frac{1}{l}\int_0^l \sigma(x)\,dx\right) dl, \tag{6}$$

where $f(l)$ is a probability density function of fibre lengthand has the following characteristics:

$$\int_0^\infty f(l)\,dl = 1; \tag{7}$$

$$\int_0^\infty f(l)\,l\,dl = \bar{l}; \tag{8}$$

$\bar{l}$ in Equation 8 denotes the average fibre length. Then the rule of mixtures can be expressed as

$$\sigma_{cu} = \bar{\sigma}V_f + \sigma'_m(1 - V_f). \tag{9}$$

Equation 9 is a modified form of Equation 2. The values of $\bar{\sigma}$ and σ_0 are not the same. However, the difference diminishes as the fibre length increases. For relatively large fibre aspect ratio it can be assumed that $\bar{\sigma} \approx \sigma_0$. Furthermore, by defining the stress concentration factor K as

$$\sigma_{max} = \sigma_{fu} = K\sigma_0$$

Equation 9 can be written as

$$\sigma_{cu} = \frac{\sigma_{fu}}{K}V_f + \sigma'_m(1 - V_f). \tag{10}$$

Consequently, the problem of short fibre composite strength is now reduced to the prediction of maximum stress concentration factor in the specimen.

2.2. Stress concentration factor

The stress concentration factor for the unidirectional fibre arrangement of Fig. 3 is difficult to evaluate in a precise manner. The following assumptions are adopted to facilitate the calculation of K: (a) fibres are of the same length, l, (b) they are arranged in rows along the axial direction, (c) the spacing between two neighbouring rows is uniform and is denoted by h (Fig. 4a) and (d) fibres with ends in the critical zone of width βl are assumed to have the ends aligned along the cross-section zz′ (Fig. 4b).

It is assumed that the fibre length l is much larger than the critical length l_c and hence, results for long fibres can be used. Following the terms used by Bader *et al.* [10], in Fig. 4a Fibres 1 and 4 are named "bridging fibres" and Fibres 2 and 3 as "ending fibres." If there are many bridging fibres surrounding the ending fibres as shown in Fig. 5a the stress concentration at point A can be calculated using the results of Hedgepeth [11] for two-dimensional problems, and Hedgepeth and Van Dyke [12] for three-dimensional problems. If the probability of finding fibre ends is high, the situation can be more closely simulated by that in Fig. 5b. In this case, a treatment similar to that used by Fukuda and Kawata [13] should be used. It is understood that although in actual composites the short fibre arrangements are quite random, Fig. 5a and b represent the typical cases in local stress magnification. The clustering of fibre ends as shown in Fig. 4b are called a "fibre end gap".

2.3. Probabilistic approach

The objective of this section is to determine the probability of finding fibre end gaps in a unidirectional system as a function of the number

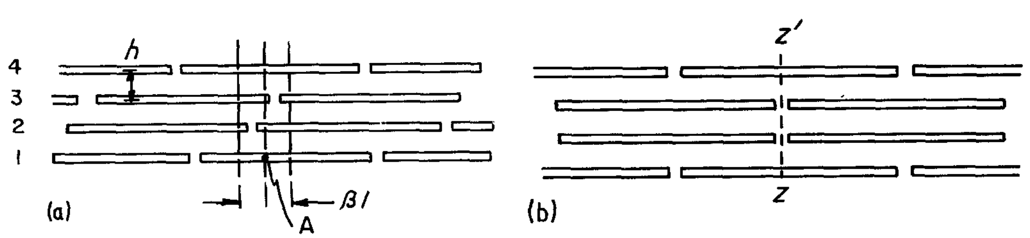

Figure 4 Model for calculating K.

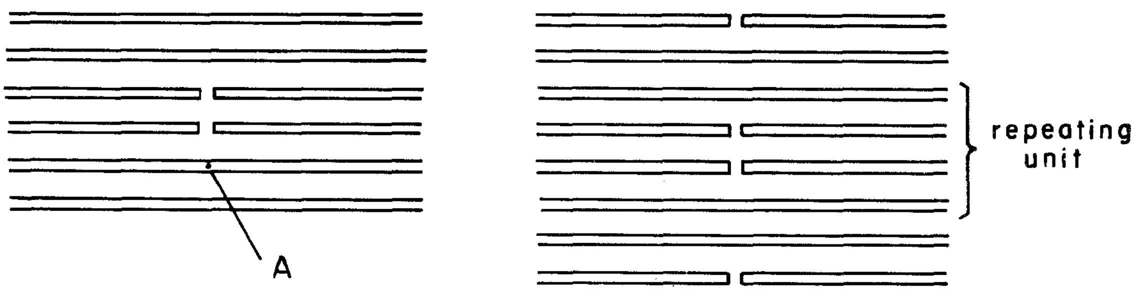

Figure 5 Examples of arrays of bridging fibres and ending fibres.

of fibre ends in the gap. The number of fibre ends in a gap appearing on a plane transverse to the fibre direction determines the stress concentration on the bridging fibres immediately surrounding the gap. In the following, a model for two-dimensional fibre arrays is first discussed and the probability functions are derived. The model is then extended to the case of three-dimensional fibre arrays.

Fig. 6 schematically shows the development of the probability function for a two-dimensional fibre arrangement. In order to simplify the discussion, firstly the probability function for a half region is demonstrated in Fig. 6. Fig. 6 depicts a gap between two short fibres aligned in the axial direction. The probability of finding an adjacent bridging fibre (denoted by $i = 1$ in Fig. 6b) is given by

$$P_1 \doteq 1 - \beta. \qquad (11)$$

Then the probability of Fibre 1 being an ending fibre (Fig. 6c) is denoted by

$$\bar{P}_1 = 1 - P_1. \qquad (12)$$

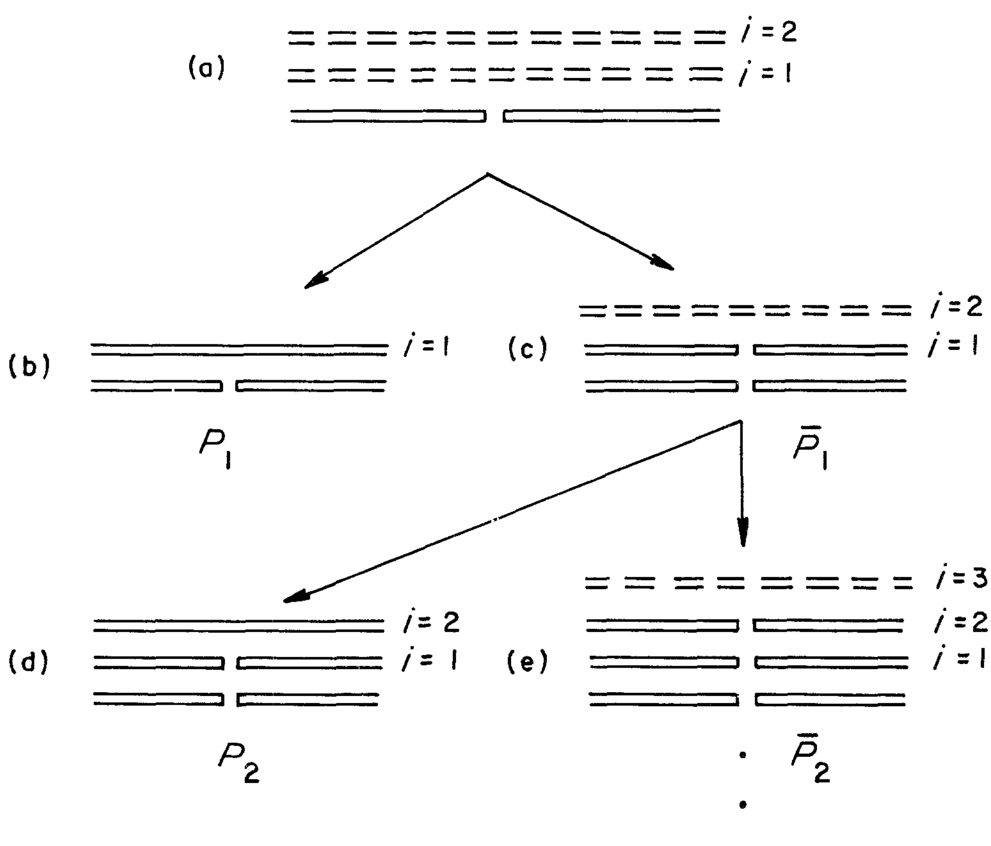

Figure 6 Probability model for finding fibre end gaps, half space.

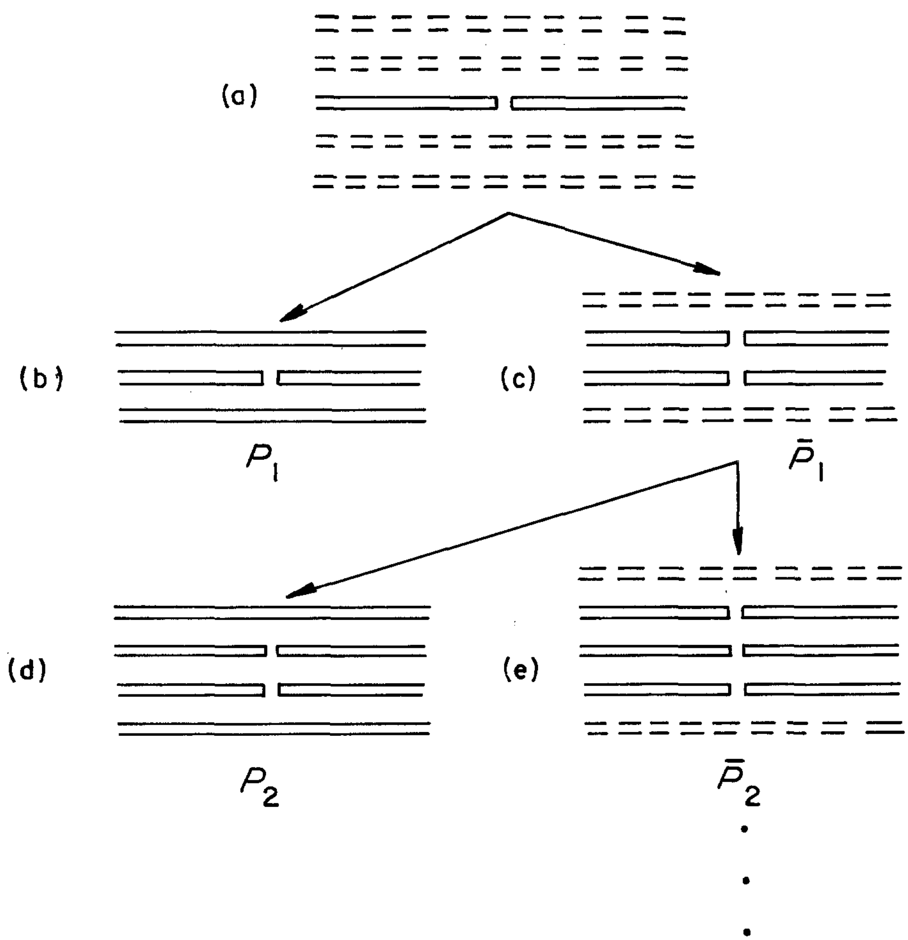

Figure 7 Probability model for finding fibre end gaps, total space.

Then the probability is derived of finding a gap containing any arbitrary number of fibre ends aligned along a plane transverse to the fibre direction. Fig. 6d shows two adjacent fibre end gaps next to a bridging fibre ($i = 2$). The probability of finding this configuration is

$$P_2 = \bar{P}_1(1-\beta). \tag{13}$$

The probability that Fibre 2 also has a gap (Fig. 6e) is denoted by $\bar{P}_2$ and it can be found by observing that

$$P_2 + \bar{P}_2 = \bar{P}_1. \tag{14}$$

Consequently,

$$\bar{P}_2 = \bar{P}_1 - P_2. \tag{15}$$

An identical reasoning can be applied to Fig. 7. Starting from one gap (Fig. 7a), the probability that both surrounding fibres are bridging fibres (Fig. 7b) is

$$P_1 = (1-\beta)^2. \tag{16}$$

The residual part

$$\bar{P}_1 = 1 - P_1 \tag{17}$$

indicates that at least one adjacent fibre is ending (Fig. 7c). Fig. 7c shows the probabilities given by both Fig. 7d and 7e. Then the probability that the situation of Fig. 7d appears is

$$P_2 = \bar{P}_1(1-\beta)^2 \tag{18}$$

and the residual

$$\bar{P}_2 = \bar{P}_1 - P_2 \tag{19}$$

indicates the situation of Fig. 7e. Finally, it can be deduced that the probability of finding a gap which consists of n ending fibres aligned along a transverse plane and enclosed on both sides by two bridging fibres (Fig. 8) is

$$P_n = \bar{P}_{n-1}(1-\beta)^2 \tag{20}$$

and the residual part is

$$\bar{P}_n = \bar{P}_{n-1} - P_n. \tag{21}$$

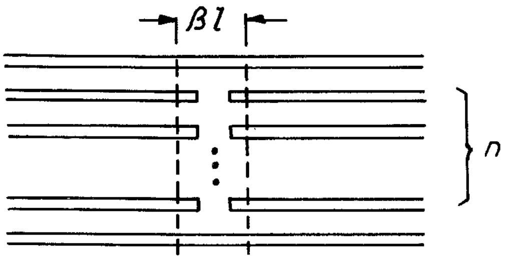

Figure 8 A fibre end gap consisting of n fibre ends.

From Equations 20 and 21

$$\bar{P}_n = \bar{P}_1\bar{P}_{n-1} = \ldots = \bar{P}_1^n \quad (22)$$

and therefore, Equation 20 can be written as

$$P_n = \bar{P}_1^{n-1}(1-\beta)^2. \quad (23)$$

It is easily shown from Equation 23 that the following relation holds

$$\sum_{n-1}^{\infty} P_n = 1. \quad (24)$$

It should be noted that in Fig. 7 the derivation begins by focussing our attention on a fibre end gap. It can be readily shown that the end result (Equation 23) is unchanged by focussing on a bridging fibre to begin with.

In the case of three-dimensional fibre arrays, the problem becomes more complex for the following reasons. First, the number of bridging fibres surrounding a fibre gap is not constant in the three-dimensional case whereas the number is always two in two-dimensional models. Fig. 9 schematically shows the cross-sectional view of bridging fibres surrounding a fibre gap based upon a hexagonal array. The number of bridging fibres is six for a gap with one ending fibre and eight for two ending fibres (Fig. 9a and b). However, the number of bridging fibres is either nine or ten for a gap with three ending fibres (Fig. 9c). The second complicating factor is that the stress concentrations of the bridging fibres are not the same. This can be seen, for example, in Fig. 9b for fibres denoted by A, B and C.

To circumvent the complexity in three-dimensional fibre arrays the following assumptions are adopted for simplifying the problem:

(1) The number of fibres bridging a fibre gap with n ending fibres is taken as small as possible. In other words, the ending fibres in a fibre gap are assumed to be packed as compactly as possible.

(2) Bridging fibres surrounding a given fibre gap all have the same stress concentration factor.

These assumptions are used as a first approxi-

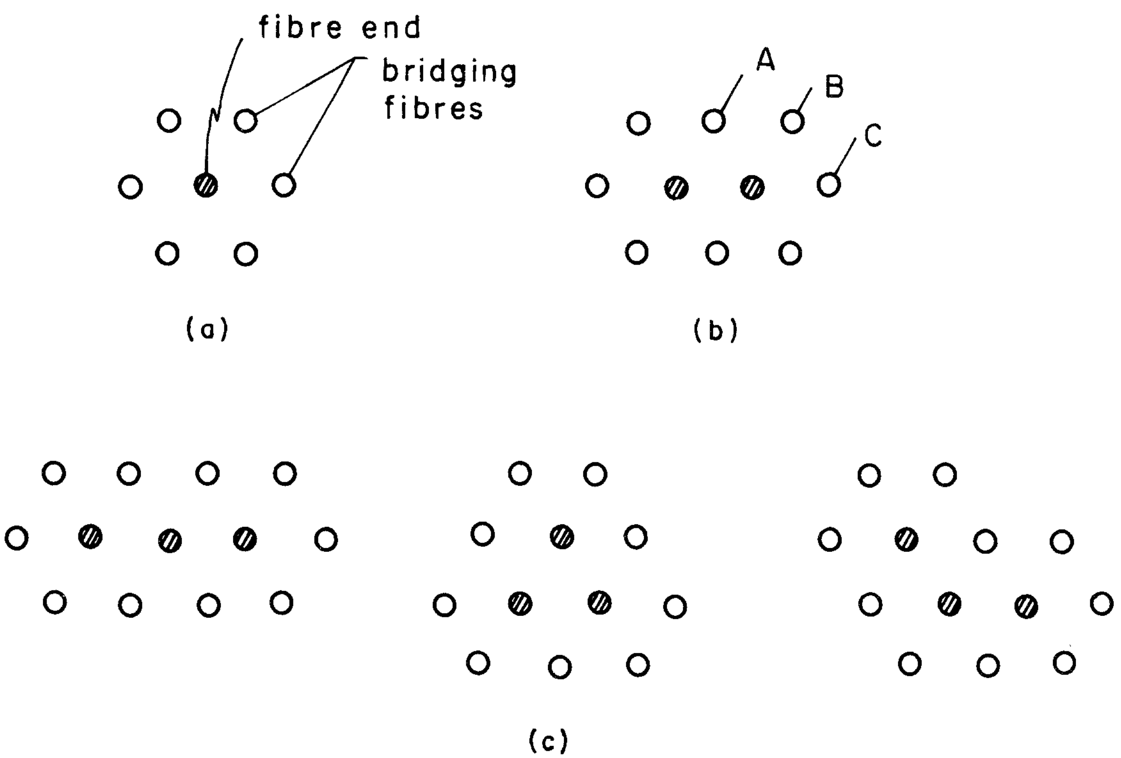

Figure 9 Fibre end gaps in hexagonal arrays.

mation. Following the discussion given for the two-dimensional fibre array model, for the three-dimensional case,

$$\begin{aligned} P_1 &= (1-\beta)^6, \quad \bar{P}_1 = 1 - P_1 \\ P_2 &= \bar{P}_1(1-\beta)^8 \\ \bar{P}_2 &= \bar{P}_1[1-(1-\beta)^8] = \bar{P}_1 - P_2 \\ P_n &= \bar{P}_{n-1}(1-\beta)^m, \quad \bar{P}_n = \bar{P}_{n-1} - P_n \end{aligned} \tag{25}$$

are obtained where m is the number of ending fibres surrounding a fibre gap of n ending fibres.

The number of short fibres. N, in a specimen of volume, V, is

$$N = \frac{4V \cdot V_f}{\pi d^2 l}, \tag{26}$$

where d and l are fibre diameter and length, respectively, and V_f is fibre volume fraction.

From the definition of P_n the quantity NP_n gives the number of fibres the end of which belong to a gap of n ending fibres. Therefore, the number of gaps of n ending fibres is NP_n/n. If NP_k/k is greater than 1, it means that such a gap of k ending fibres occurs frequently in the model. Let the maximum value of k which satisfies the condition $NP_k/k > 1$ be denoted by k_0. It can be expected that there is at least one group of k_0 neighbouring fibres forming a fibre gap in the specimen. Furthermore, there is no need to consider the gaps with less than k_0 fibre ends, since the stress concentration would be smaller and hence, less critical in fracture initiation.

By taking into account the probabilities of finding fibre gaps with the number of adjacent ending fibres k greater than or equal to k_0, Equation 10 can be rewritten as follows

$$\sigma_{cu} = \sigma_{fu} V_f \left[\sum_{j=k_0+1}^{\infty} \frac{1}{K_j} \frac{NP_j}{j} + \frac{1}{K_{k0}} \left(1 - \sum_{j=k_0+1}^{\infty} \frac{NP_j}{j}\right) + \sigma'_m (1 - V_f) \right]. \tag{27}$$

It is understood that σ_c in Equation 27 is the average strength of many test specimens.

2.4. Numerical results

Numerical calculations of short fibre composite strength based upon the above theory have been carried out. The result of Hedgepeth [11] is adopted for the stress redistribution near fibre discontinuities of unidirectionally arrayed two-dimensional model. According to Hedgepeth [11] for a two-dimensional and unidirectional fibre array, the stress concentration factor of a fibre adjacent to r discontinuous fibres is given by

TABLE I Hexagonal array stress concentration factors [12]

Number of discontinuous fibres, r	Maximum stress concentration factor
1	1104
7	1410
19	1630
37	1874

$$K_r = \frac{4}{3} \times \frac{6}{5} \ldots \times \left(\frac{2r+2}{2r+1}\right). \tag{28}$$

This expression is used in Equation 27. In the case of the three-dimensional model, Hedgepeth and Van Dyke [12] obtained the stress concentration factor for symmetrical arrangement of discontinuous fibres. Their results for the hexagonal array models are given in Table I. As shown in Fig. 9, our models are not necessarily symmetrical with respect to fibre ends. However, the values of Table I were adopted as a first approximation. Linear interpolation was used to estimate the stress concentration factor for an intermediate number of discontinuous fibres, that is, $r = 2, 3 \ldots 6, 8, 9 \ldots 18, 20, 21 \ldots$.

Equation 27 was rearranged as follows

$$\sigma_{cu}/\sigma'_m = \sigma_{fu}/\sigma'_m V_f F + (1 - V_f), \tag{29}$$

where F can be easily deduced from Equation 27. The factor F is calculated by assuming $l_c = 0.1$ mm, $d = 0.01$ mm and $V = 400\,\text{mm}^3$. Fig. 10 shows the relation between F and the fibre length, l, for both two- and three-dimensional analysis. It should be noted that F decreases slightly with increasing V_f. In the case of three-dimensional fibre array the value of F in the series expression (Equation 27) converges very slowly at very small fibre length. This is attributed to the fact that the extremely short fibre length range is not suitable for the present theory. Hence a broken line is drawn in Fig. 10 for the range of fibre lengths between 0.5 and 1 mm. Both Equations 2 (rule of mixtures) and 4 (Riley's solution) can be rewritten as Equation 29 and these values of F are also shown in Fig. 10. Taking into consideration the effect of fibre end gaps, our results predict a smaller F value than those of the rule of mixtures and Riley's solution.

Although we do not have the experimental

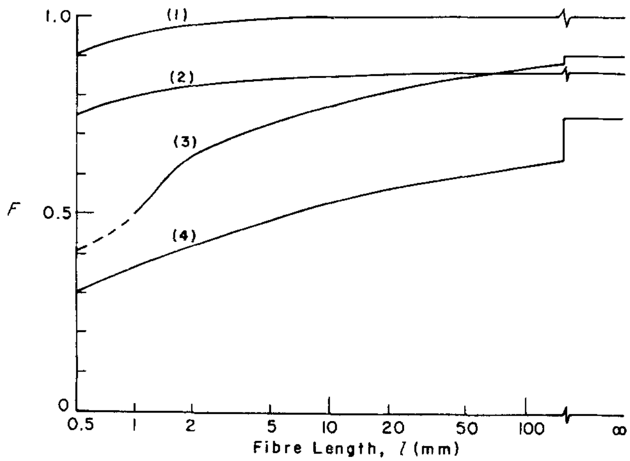

Figure 10 Reinforcement factor F against fibre length. (1) rule of mixtures, (2) Riley's solution, (3) and (4) present analysis, (3) three-dimensional array, (4) two-dimensional array.

value of σ_{fu}/σ'_m, it is equivalent to E_f/E_m if both fibre and matrix are assumed to be linearly elastic. In Fig. 11 the relation of composite strength against volume fraction of fibre at $E_f/E_m = 35.2$ [14] and $l = 0.5$ mm is shown. Our theory

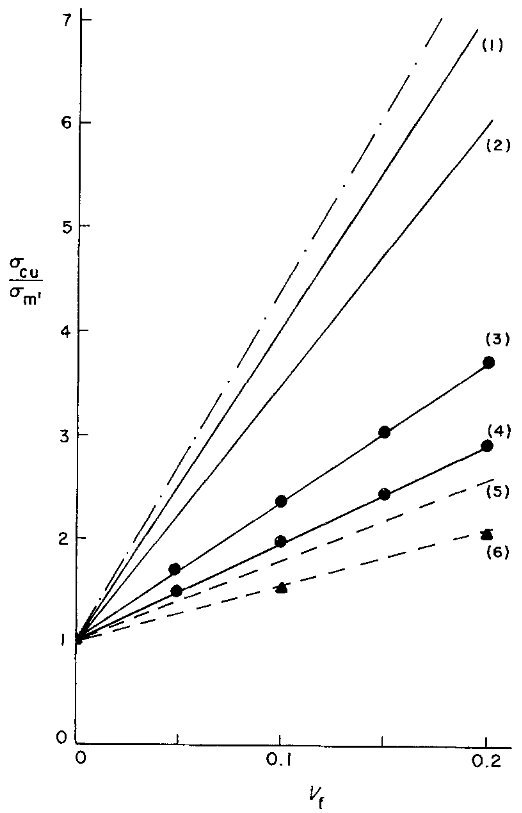

Figure 11 Strength of short fibre composites as a function of V_f with $\bar{l} = 0.5$ mm, (1) rule of mixtures, (2) Riley's solution [8], (3) and (4) present analysis, (3) three-dimensional, (4) two-dimensional, (5) and (6) modified value at $C = 0.59$, (5) three-dimensional, (6) two-dimensional. —·— rule of mixtures for $l = \infty$, ▲ experimental data, LGN [9].

is based on the assumption of unidirectional fibre array. In actual injection-moulded composite materials, fibres are not perfectly aligned. If the orientation factor $C = 0.59$ [14] is multiplied to the first term of Equation 29, the broken lines in Fig. 11 can be obtained. The experimental data [9] are represented by ▲ in Fig. 11. The fibre length of 0.5 mm used in the experimental work of Curtis *et al.* [9] is too short for the present theory to be applied in a satisfactory manner. Better agreement can be obtained for larger fibre aspect ratios and with more information on fibre orientation distribution.

3. Discussions and conclusions

(1) The present theory adopted the concept of a "critical zone" in the failure of short fibre composites. The stress redistribution in the critical zone due to stress concentrations has been examined.

(2) The stress concentrations at the ends of short fibres are evaluated by considering the size of a fibre end gap as a function of the number of fibre ends forming the gap.

(3) The occurrence of fibre end gaps of different sizes is predicted based upon a probabilistic approach. Unidirectional short fibre composites can be calculated from the gap size and corresponding stress concentration factor.

(4) Quantitative comparisons of the theory with experiment is difficult at the present time particularly because of the lack of information on fibre length and orientation distributions, as well as fibre critical length in actual short fibre composite systems.

Acknowledgements

This work was supported by the US Department of Energy under Contract DE-AC02-79ER10511. We also thank M. G. Bader for helpful discussions.

References

1. T. W. CHOU and A. KELLY, *Mater. Sci. Eng.* **25** (1976) 35.
2. *Idem, Ann. Rev. Mater. Sci.* **10** (1980) 229.
3. J. R. VINSON and T. W. CHOU, "Composite Materials and Their Use in Structures" (Elsevier-Applied Science, London, 1975).
4. C. ZWEBEN, *AIAA J.* **6** (1968) 2325.
5. H. FUKUDA and K. KAWATA, *Trans. Jap. Soc. Compos. Mater.* **2** (1976) 59.
6. *Idem, Fibre Sci. Tech.* **10** (1977) 53.
7. K. P. OH, *J. Compos. Mater.* **13** (1979) 311.
8. V. R. RILEY, *ibid.* **2** (1968) 436.
9. P. T. CURTIS, M. G. BADER and J. F. BAILEY, *J. Mater. Sci.* **13** (1978) 377.
10. M. G. BADER, T. W. CHOU and J. QUIGLEY, in "New Developments and Applications in Composites," edited by D. Wilsdorf (The Metallurgical Society-American Institute of Mining Metallurgy and Petroleum Engineering, New York, 1979).
11. J. M. HEDGEPETH, NASA TN D-882 (1961).
12. J. M. HEDGEPETH and P. VAN DYKE, *J. Compos. Mater.* **1** (1967) 294.
13. H. FUKUDA and K. KAWATA, *Fibre Sci. Tech.* (1981).
14. M. G. BADER, private communication, (1980).

Received 6 August and accepted 10 November 1980.